Радиофизика и радиоастрономия, 1997, т. 2, №3, 302-317

Efficient Technique to Solution of SIE in Scattering Theory

Zinoviy Nazarchuk, Oleg Ovsyannikov

Karpenko Physico-Mechanical Institute of the National Academy of Sciences of Ukraine
5 Naukova St., Lviv 290601, Ukraine, Fax: (380) 322 649427, E-mail: nazarchuk@ah.ipm.lviv.ua

Efficient numerical approach proposed to solution of the scalar diffraction problem for arbitrary shaped cylindrical screens is considered. Treatment is based on direct numerical solution of the singular integral equations of the problem.

Keywords: scattering theory, singular integral equations, numerical methods, stratified medium.

Introduction

An analysis of electromagnetic wave scattering by different type of inhomogeneities in the plane stratified media is one of the interesting problems in radio science [1-4], geophysics [5-7], non-destructive testing [8,9] and the other applications. In the resonance region - the most difficult case for theoretical investigation - the integral equation technique is widely used in solving of the corresponding diffraction problems. For heterogeneous structures including different cylinders such equations were formulated regarding unknown surface current densities [10,11] or internal fields [12-15]. Numerical investigation of electromagnetic scattering by resonant screens in open planar stratified media has been carried out in the case of strips [16,17], circular cylinder with a slot [18,19], combination of them [20]. The integral equation technique was extended also for analysis and design of multilayer printed circuits and antennas [21-25]. The paper [26] reviews recent works by a number of investigators in this field. Note, that the moment method [27] is widely used under numerical treatment of the corresponding integral equations. Sometimes (for example, in the case of resonance mode excitation) such approach leads to a large algebraic system and could not reach a sufficient accuracy. Similar problem appears under investigation of the other resonant structures. A diffraction grating is well-known representative of such structures due to its important role in different electronic equipment design. Rigorous mathematical approaches are very useful in this case to state the physical properties of a scattered field. A simple grating of strips or circular cylinders with or without slot is usually explored as a classical testing ground of these techniques (see ex. [28-33]). In comparison with single element array which diffraction properties are sufficiently established the multilayered grating has additional waveguide features [34]. In both cases arbitrary curvature of grating's element destroys the implementation of such rigorous approaches and needs of numerical method's usage.

The present paper's aim is to outline a general numerical approach to accurate solution of wide class diffraction problems for arbitrary cylindrical screen's system. The approach is based on singular integral equations' technique. We illustrate this approach to the screens in an open planar waveguide as well as to a multilayer diffraction grating. The features of the proposed algorithms are: application of the potential method in boundary integral equations [29]; direct numerical treatment of the obtained singular integral equations using the interpolation-quadrature technique [35]; manner of Green functions calculation by contour integration and polynomial approximation [36]. We exemplify the algorithm's serviceability and validity by solution of scattering problem in the case of two resonance cylindrical screens located in a dielectric slab.

Statement of problem

Let planes $z=0$ and $z=-d$ form the boundaries of stratified medium. Assume that the upper half-space S_1, the slab S_2 and the lower half-space S_3 have dielectric permittivities ε_1, ε_2, ε_3 and magnetic permeabilities μ_1, μ_2, μ_3, correspondingly. Note, if we put $\varepsilon_2=\varepsilon_3$, $\mu_2=\mu_3$, then the slab' thickness tends to infinity. In the case of $\varepsilon_1=\varepsilon_2=\varepsilon_3$, $\mu_1=\mu_2=\mu_3$ we obtain a homogeneous medium. Let the slab consists of a system of N open, infinitely thin and perfectly conducting cylindrical screens as well as a homogeneous dielectric cylinder (rod) with dielectric permittivity ε_0 and magnetic permeability μ_0. We suppose that the structure is uniform in the z-direction of Cartesian coordinate system xyz (Fig.1).

The arbitrary smooth contours L_k, $k=\overline{1,N}$ and L_0 form a cross section of the screens and cylinder by xOy plane. We designate a domain inside of curve L_0 as S_0. In the plane xOy we consider an arbitrary two-dimensional wave with time factor $\exp(-i\omega t)$ (ω is an angular frequency) as illumination of the described above structure. Introduce now the corresponding wave numbers χ_i:

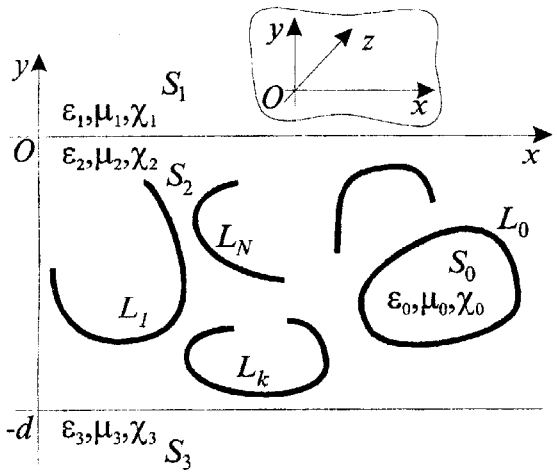

Fig. 1. *The geometry of the problem*

$$\chi_i = \omega\sqrt{\varepsilon_i\mu_i};\ i=\overline{0,3}.$$

Then the scattered field satisfies the Helmholtz equation

$$\Delta\begin{Bmatrix}E\\H\end{Bmatrix}+\chi_i^2\begin{Bmatrix}E\\H\end{Bmatrix}=0$$

(E and H are electric and magnetic field's components). Our problem is to determine the solution of this equation with continuity conditions for tangential components on the boundaries of domains S_i, $i=\overline{0,3}$:

$$\left[\vec{n},E_i\right]\Big|_{S_i\cap S_j}=\left[\vec{n},E_j\right]\Big|_{S_i\cap S_j},$$

$$\left[\vec{n},H_i\right]\Big|_{S_i\cap S_j}=\left[\vec{n},H_j\right]\Big|_{S_i\cap S_j},\ i,j=\overline{0,3}$$

as well as with the following conditions on the screens:

$$\left[\vec{n},E_i\right]\Big|_{L_k}=0,\ k=\overline{1,N}$$

($\vec{n}$ is a normal to the corresponding boundary).

For solution uniqueness we demand that the waves which propagate from infinity (except exciting one) are absent. In addition we suppose that the field components satisfy to Meixner's edge condition at screen ribs.

Green's function

To reduce our problem to the integral equations we use the method of potential. As far as the initial problem could be separated into two cases:

- the case of E-polarization when electric component of excitation wave is parallel to the axis Oz:

$$\vec{E}\left(0,0,E^*+E^s\right),\ \vec{H}\left(H_x,H_y,0\right),$$

$$H_x=-\frac{i}{\mu\omega}\left(\frac{\partial}{\partial y}E^*(x,y)+|\chi_2|h_x\right),$$

$$h_x=\frac{1}{|\chi_2|}\frac{\partial}{\partial y}E^s(x,y),$$

$$H_y=\frac{i}{\mu\omega}\left(\frac{\partial}{\partial x}E^*(x,y)+|\chi_2|h_y\right),$$

$$h_y=\frac{1}{|\chi_2|}\frac{\partial}{\partial x}E^s(z);$$

- the case of H-polarization when magnetic component of excitation wave is parallel to the axis Oz:

$$\vec{H}\left(0,0,H^*+H^s\right),\vec{E}\left(E_x,E_y,0\right),$$

$$E_x=\frac{i}{\varepsilon\omega}\left(\frac{\partial}{\partial y}H^*(x,y)+|\chi_2|e_x\right),$$

$$e_x=\frac{1}{|\chi_2|}\frac{\partial}{\partial y}H^s(x,y),$$

$$E_y=-\frac{i}{\varepsilon\omega}\left(\frac{\partial}{\partial x}H^*(x,y)+|\chi_2|e_y\right),$$

$$e_y=\frac{1}{|\chi_2|}\frac{\partial}{\partial x}H^s(x,y).$$

So, we consider these cases separately. The superscripts "*" and "s" (here and below) denote components of initial and scattered field.

Let us find the Green function G of the problem as a solution of inhomogeneous Helmholtz equation in the following form

$$\left(\frac{\partial^2}{\partial x^2}+\frac{\partial^2}{\partial y^2}\right)G(x,y,x_0,y_0)+$$

$$+\chi_i^2G(x,y,x_0,y_0)=-\delta(x-x_0,y-y_0)$$

($\delta(x-x_0,y-y_0)$ is Dirack' delta function). We take into account that function G satisfies following conditions on interfaces between S_1 and S_2 domains:

$$G_1^E(x,y+0)\Big|_{y=0}=G_2^E(x,y-0)\Big|_{y=0},$$

$$\frac{1}{\mu_1}\frac{\partial G_1^E(x,y+0)}{\partial y}\Big|_{y=0}=\frac{1}{\mu_2}\frac{\partial G_2^E(x,y-0)}{\partial y}\Big|_{y=0}$$

(E-polarization);

$$G_1^H(x,y+0)\Big|_{y=0}=G_2^H(x,y-0)\Big|_{y=0},$$

$$\frac{1}{\varepsilon_1}\frac{\partial G_1^H(x,y+0)}{\partial y}\bigg|_{y=0} = \frac{1}{\varepsilon_2}\frac{\partial G_2^H(x,y-0)}{\partial y}\bigg|_{y=0}$$

(H-polarization).

Similar conditions should be satisfied at the boundary $y=-d$:

$$G_2^E(x,y+0)\big|_{y=-d} = G_3^E(x,y-0)\big|_{y=-d},$$

$$\frac{1}{\mu_2}\frac{\partial G_2^E(x,y+0)}{\partial y}\bigg|_{y=-d} = \frac{1}{\mu_3}\frac{\partial G_3^E(x,y-0)}{\partial y}\bigg|_{y=-d}$$

(E-polarization);

$$G_2^H(x,y+0)\big|_{y=-d} = G_3^H(x,y-0)\big|_{y=-d},$$

$$\frac{1}{\varepsilon_2}\frac{\partial G_2^H(x,y+0)}{\partial y}\bigg|_{y=-d} = \frac{1}{\varepsilon_3}\frac{\partial G_3^H(x,y-0)}{\partial y}\bigg|_{y=-d}$$

(H-polarization).

Additionally, the Green function G has to satisfy certain (see above) condition at the infinity. In the cases of E- and H-polarization we get two Green functions [37]. We can write them in the domain S_1 and S_2 as follows:

$$G_1^{E,H}(x,y,x_0,y_0) = \sum_{p=1}^{2}\frac{1}{4\pi}\times$$

$$\times\int_{-\infty}^{+\infty}\frac{f_p\exp\left[\gamma_p\nu_2 - y\nu_1 + i\xi\{x-x_0\}\right]}{g}d\xi,\ p=1,2,$$

$f_i=2(\nu_2 p_{13}+\nu_3 p_{23})$, $\gamma_1=y_0$,

$f_2=2(\nu_2 p_{13}-\nu_3 p_{23})$, $\gamma_2=-2d-y_0$,

$-d\le y_0\le 0$, $y\ge 0$;

$$G_2^{E,H}(x,y,x_0,y_0) =$$

$$=\frac{1}{4}H_0^{(1)}(\chi r) + S_2^{E,H}(x-x_0,y,y_0),$$

$$S_2^{E,H}(x,y,y_0) =$$

$$\sum_{p=1}^{4}\frac{1}{4\pi}\int_{-\infty}^{+\infty}\frac{g_p\exp\left[\theta_p\nu_2 + i\xi x\right]}{\nu_2 g}d\xi,\ p=\overline{1,4},$$

$-d\le y,\ y_0\le 0$,

$g_1=(\nu_2 p_{13}-\nu_1 p_{23})(\nu_2 p_{13}+\nu_3 p_{23})$, $\theta_1=y_0+y$,

$g_2=(\nu_2 p_{13}-\nu_1 p_{23})(\nu_2 p_{13}-\nu_3 p_{23})$, $\theta_2=-2d+y_0-y$,

$g_3=(\nu_2 p_{13}+\nu_1 p_{23})(\nu_2 p_{13}-\nu_3 p_{23})$, $\theta_3=-2d-y_0-y$,

$g_4=g_2$, $\theta_4=-2d-y_0+y$,

$g=(\nu_2 p_{13}+\nu_1 p_{23})(\nu_2 p_{13}+\nu_3 p_{21})-$

$-(\nu_2 p_{13}-\nu_1 p_{23})(\nu_2 p_{13}+\nu_3 p_{21})\exp[-2d\nu_2]$.

Here $H_0^{(1)}(z)$ is Hankel function, $p_{ij}=\mu_i\mu_j$ (E-polarization) or $p_{ij}=\chi_i^2\chi_j^2$ (H-polarization); $\nu_j=\sqrt{\xi^2-\chi_j^2}$; $\Re\{\nu_\varphi\}\ge 0$; $i,j=\overline{1,3}$. Similar expressions can be easily written in the domain S_3.

First we consider the simplest case of the problem for homogeneous medium. Suppose that the incident plane wave propagates at the angle β to the axis Oy. Let the system of N screens forms an infinite grating with period d (Fig. 2). In this case for the E-polarization we have the following well known representation of the Green function:

$$G_g^E(t_k,z) = \frac{i}{4}H_0^{(1)}\left(\chi|t_k-z|\right) +$$

$$+\frac{i}{4}\sum_{\substack{u=-\infty\\ u\ne 0}}^{+\infty}H_0^{(1)}\left(\chi|t_k+ud-z|\right).$$

As far as our problem does not depend on z coordinate we use this symbol (here and below) to denote a complex value $z=x+iy$. Then $\bar{z}=x-iy$ designates a complex conjugate value. If point z belongs to contour L_k (L) we put $z\equiv t_k=x_k+iy_k$ ($z\equiv t$).

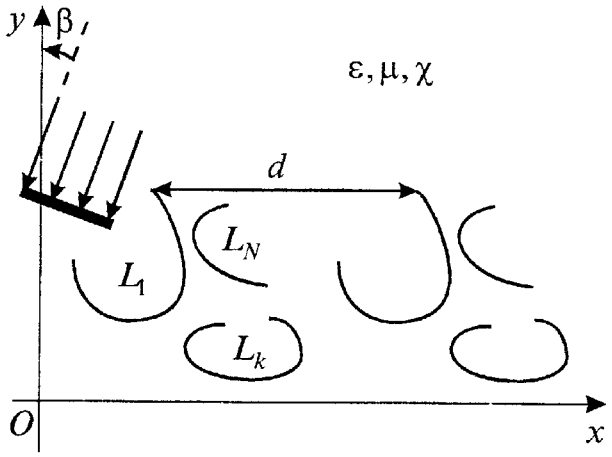

Fig. 2. *Infinite gratings in the field of plane wave*

As it is well known the above series are weak to converge. For its calculation we propose to use the familiar integral representation of Hankel function [38]:

$$\frac{i}{4}H_0^{(1)}\left(\chi|t-z|\right) = \frac{1}{4\pi}\int_\Gamma\frac{1}{\nu}e^{-\Im\{t-z\}\nu+i\xi\Re\{t-z\}}d\xi,$$

$$\nu=\sqrt{\xi^2-\chi^2},\ \Re\{\nu\}\ge 0,$$

$$\Im\{\nu\}<0,\ \Im\{\xi\}\ge 0,\ 0\le\Re\{\xi\}\le\chi,\ \xi\in\Gamma_m.$$

Here the contour Γ is chosen according to the Fig. 3, $\Lambda_\pm$ are cuts on the complex plane ξ.

Substitution of the last formula into the Green function representation yields

$$G_g^E(t_k,z)=\frac{i}{4}H_0^{(1)}\left(\chi|t_k-z|\right)+$$
$$+\frac{1}{4\pi}\sum_{u=1}^{+\infty}e^{-i\chi du\sin\beta}\int_{\Gamma_m}\frac{1}{\nu}e^{-|\Im\{t_k-z\}|\nu-i\xi\Re\{t_k-ud-z\}}d\xi+$$
$$+\frac{1}{4\pi}\sum_{u=1}^{+\infty}e^{i\chi du\sin\beta}\int_{\Gamma_m}\frac{1}{\nu}e^{-|\Im\{t_k-z\}|\nu-i\xi\Re\{t_k+ud-z\}}d\xi.$$

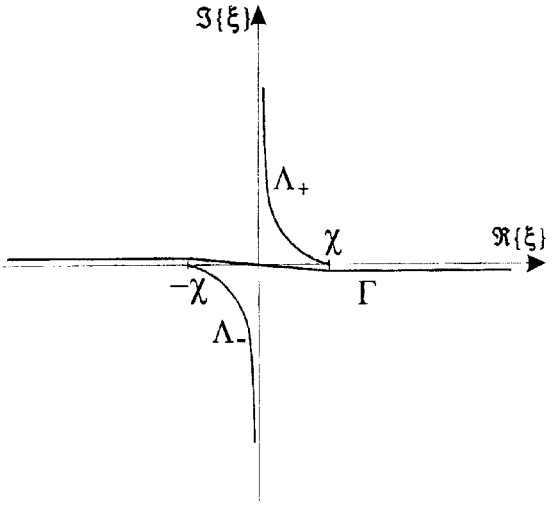

Fig. 3. *Integration path for Hankel function integral representation*

Note that it is impossible to move the sum sign into integral (under such action the sums diverge in the fourth quadrant of complex ξ-plane). To do it we have to change the integration path according to Fig. 4.

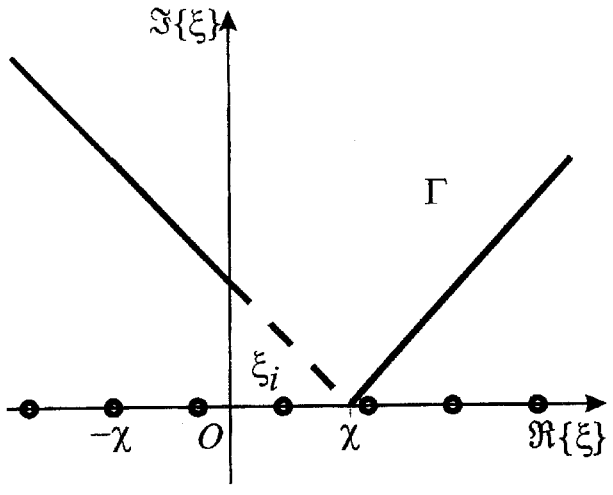

Fig. 4. *Integration path for Green function of periodic problem*

Hidden line of the path signs the part where $\Re\{\nu\}\le 0$. Thus, after carrying out some manipulations we lead to

$$G_g^E(t_k,z)=\frac{i}{4}H_0^{(1)}\left(\chi|t_k-z|\right)+\sum_{p=1}^{2}S_p(t_k,z,d,\beta),$$

$$S_p(t_k,z,d,\beta)=\frac{1}{4\pi}\exp[qi\chi d\sin\beta]\times$$
$$\times\int_{\Gamma_m}\frac{\exp\left[-|\Im\{t_k-z\}|\nu+qi\xi\Re\{t_k+qd-z\}\right]}{\nu\left(1+qe^{id(\xi+q\chi\sin\beta)}\right)}d\xi,$$

$q=(-1)^p$.

It is easy to see that there are Cauchy's type singularities of the integrands at the nodes $\xi_i=q\pi/d-q\chi\sin\beta$. We denote them by nodes on the Fig. 4.

Let us consider the numerical algorithm for Green function calculation. It is easy to see that the Green function consists of two kinds summands. The first kind is a fundamental solution of Helmholtz equation (a free space Green function) and consists a logarithmic singularity. The second one is a series of Sommerfeld type integrals. The last integrals are regular functions. Nevertheless they cause well known difficulties during the Green function calculation.

Let us write a general form of the Sommerfeld type integrals for stratified medium by mean of the following formula [39]

$$I(\alpha,\beta)\equiv\int_{-\infty}^{+\infty}\frac{\varphi(\xi)}{\nu_2}\exp(-\alpha\nu_2+i\xi\beta)d\xi. \quad (1)$$

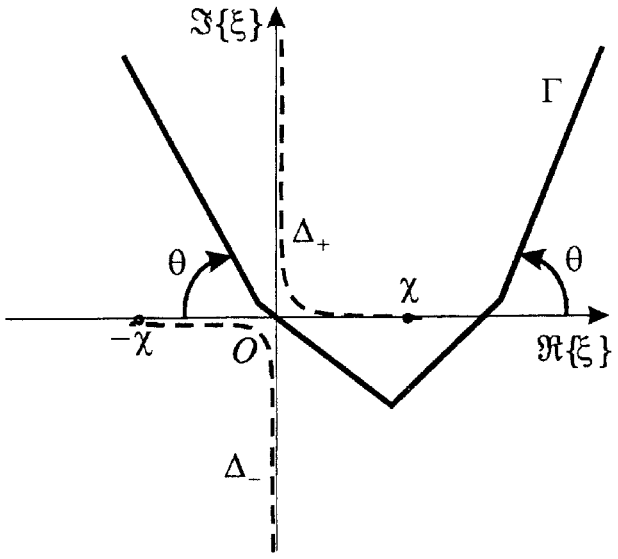

Fig. 5. *Integration path for Sommerfeld type integrals*

We propose to use some integration path Γ according to the Fig. 5. The angle θ is chosen according to relation

$$\Im[-\alpha\nu_2+\imath\beta\xi] \underset{\xi\to\infty}{\sim} \text{const}, \ \text{tg}(\theta)=\beta/\alpha, \ \xi\in\Gamma. \quad (2)$$

Condition (2) ensures the fastest decay of the integrand (1) and avoids its oscillation.

If the losses of stratified medium are absent then the waves are not damped and can propagate to infinity in the domain S_2. Mathematically, the advent of an own waveguide mode corresponds to residue appearance on the real interval $[0;\chi_2]$. We can write this condition in the following form

$$g(\xi_i)=0; \quad g'(\xi_i)\neq 0, \quad i=\overline{1,n}. \quad (3)$$

Here n_z is a number of zeros of the function $g(\xi)$. Actually, n_z is the same as a number of waveguide modes.

Let us consider an asymptotic behavior of the Green function at $x\to\infty$. As well as at $x\to\infty$ the integrands in the fourth quarter tend to infinity we have to change an integration path according to Fig. 6 in the case when $n_z\neq 0$.

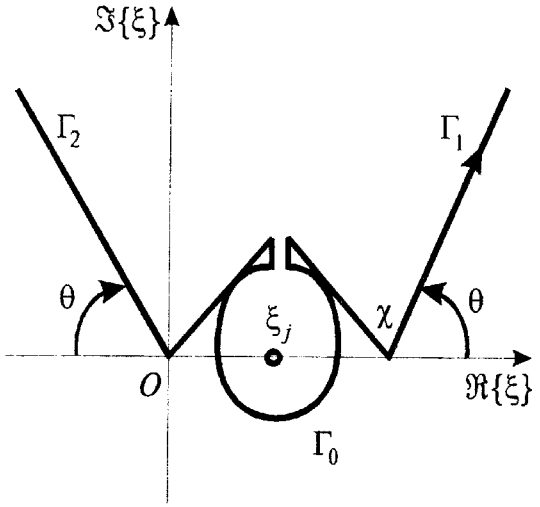

Fig. 6. *Integration path for Sommerfeld type integrals at* $\xi\to\infty$

It is obvious that integrals over $\Gamma_1\cup\Gamma_2$ tend to zero and integrals over Γ_0 are equal to sum of the residuals at points ξ_i, $i=\overline{1,n_z}$. Hence, the asymptotic expansion of Green function can be written as

$$G_1^{E,H}\left(x=\rho\sin\varphi, y=\rho\cos\varphi, x_0, y_0\right) \underset{\rho\to\infty}{\equiv}$$

$$\equiv G_{1\infty}^{E,H}(t)=\sum_{j=1}^{n_z} P_{1\infty}^{E,H}\left(\xi_j\right)\exp\left[\Im\left\{\nu_1\left(\xi_j\right)\right\}y+i\xi_j x\right]+$$

$$+L_{1\infty}^{E,H}(t,\varphi)\sqrt{\frac{1}{2\pi\chi_1\rho}}\sin\varphi\exp\left(i\chi_1\rho-i\pi/4\right);$$

$$G_2^{E,H}\left(x,y,x_0,y_0\right) \underset{x\to\infty}{\equiv}$$

$$\equiv G_{2\infty}^{E,H}(t)=\sum_{j=1}^{n_z} P_{2\infty}^{E,H}\left(\xi_j\right)\exp\left[i\Im\left\{\nu_2\left(\xi_j\right)\right\}y\right]e^{i\xi_j x}.$$

Here $L_{1\infty}^{E,H}(t,\varphi)$ is known function that depends only on coordinates; $P_{1,2\infty}^{E,H}\left(\xi_j\right)$ are coefficients that depend on number of modes.

It is easy to see that the Green function representation for the upper half-space has two components. The first one is a function that vanishes at infinity. The second one is undamped function and has exponential behavior at $y\to\infty$. The Green function representation in the domain S_2 has only undamped waveguide modes.

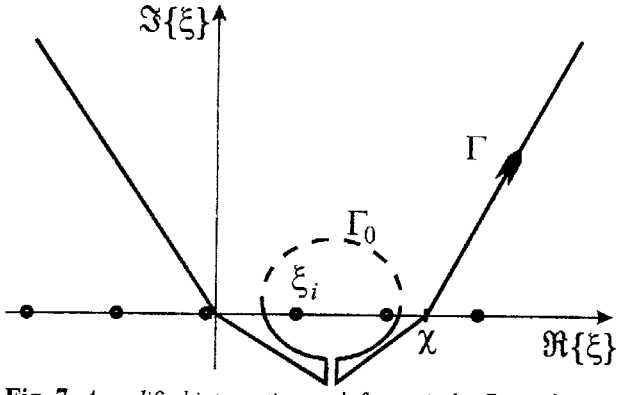

Fig. 7. *A modified integration path for periodic Green function*

In the case of periodic Green function we have to change our approach as far as the Green function is defined on the grating period and is periodical function of x-coordinate. So it is necessary to consider its asymptotic behavior when y tends to infinity. For this reason we have to change an integration path because on its hidden part the integrands grow to infinity. To do it we choose an integration path according to Fig. 7.

As in previous case, integral on the contour Γ_0 gives us the residual contribution. An integral over the contour Γ_m vanishes at infinity. So we obtain the following formula

$$G_g^E\left(t_k,z\right)\Big|_{y\to\pm\infty}=\sum_{m=-n_1}^{n_2}\frac{i}{2\chi d\cos\beta_m}\times$$

$$\times e^{i\chi\left(\pm\cos(\beta_m)\Im\{z-t_k\}+\sin(\beta_m)\Re\{z-t_k\}\right)}, \quad (4)$$

$$\sin\beta_m = \sin\beta + 2\pi m/(\chi d),$$

$$\cos\beta_m = \sqrt{\cos^2\beta - \left(\frac{2\pi m}{\chi d}\right)^2 - \frac{4\pi m\sin\beta}{\chi d}},$$

$$\Im\{\cos\beta_m\} \ge 0, n_p = \frac{\chi d}{2\pi}\left(1+(-1)^p\sin\beta\right),\ p=1,2.$$

It is easy to see that number of the modes depends on the excitation frequency. Angle of the plane wave incidence just shifts these modes.

Now we are ready to calculate the Sommerfeld type integrals but unfortunately it is too hard work. To make it easier we propose to use an interpolating polynomial. There are many different approaches to build such polynomials and may be it is not so easy to choose an appropriate one.

Let we need to interpolate a function that passes the points $(x_1,f(x_1))$, $(x_2,f(x_2))$,... $(x_n,f(x_n))$ [40].

Let us put

$$l_{j,n}(x) = l_j(x) = \frac{(x-x_1)\ldots(x-x_{j-1})(x-x_{j+1})\ldots(x-x_n)}{(x_j-x_1)\ldots(x_j-x_{j-1})(x_j-x_{j+1})\ldots(x_j-x_n)},$$

$$j=\overline{1,n},\ n\ge 1.$$

This expression is called as the fundamental polynomial for interpolation function $f(x)$ at nodes $x_1,\ldots, x_n$. Then

$$L_{n-1}(x) = f(x_1)l_1(x) + f(x_2)l_2(x) + \ldots + f(x_n)l_n(x)$$

is a polynomial of degree at most $n-1$ that passes through the points in question. This polynomial is unique one that interpolates $f(x)$ at $x_1,\ldots, x_n$. It is called as Lagrange' polynomial (to function $f(x)$ at nodes $x_1,\ldots, x_n$ from X). At the end, we have to choose the nodes X of the polynomial.

The following question arises: how good an approximation by mean of these polynomials is? It is easy to show that [41]

$$\left\|f(x)-L_k(x)\right\| = \max_{-1\le x\le 1}\left|f(x)-L_k(x)\right| \le$$

$$\le E_k\left(f(x)\right)\left[1+\max_{-1\le x\le 1}\sum_{j=1}^{k+1}\left|l_j(x)\right|\right],\ k=\overline{0,\infty}, \quad (5)$$

Here

$$E_k\left(f(x)\right) = \max_{-1\le x\le 1}\left|p^*(x)-f(x)\right|,$$

$p^*(x)$ is polynomial of the best approximation,

$$\lambda_{k+1}(X,x) = \sum_{j=1}^{k+1}\left|l_j(X,x)\right|$$

is called as $k+1$ order Lebesgue function of X. Note that it does not depend on $f(x)$. The quantity

$$\Lambda_{k+1}(X) = \max_{-1\le x\le 1}\lambda_{k+1}(X,x)$$

is called as the Lebesgue constant of order $k+1$.

The formula (5) shows that the smaller is $\Lambda_{k+1}(X)$, the closer the sequence of Lagrange interpolating polynomials at the nodes X is to the uniform approximation of the function f.

So let us introduce the Chebyshev polynomials of the first kind:

$$T_n(x) = \cos(n\arccos x),$$

where $-1\le x\le 1,\ 0\le\arccos x\le\pi,\ n\ge 0$.

The polynomial $T_n(x)$ has zeros which can be expressed according to the formula

$$x_k = \cos\left(\frac{2k-1}{2n}\pi\right),\ k=\overline{1,n}.$$

The point of this digression on the topic of polynomial interpolation is that the zeros of the Chebyshev polynomials of the first kind provide a grid of nodes with "small" Lebesgue constants.

Let us build the Lagrange interpolation polynomial for the integral $I(\xi,\psi=\text{const})$ from (1) at zeros of the Chebyshev polynomial of the first kind. It is obvious that

$$I(\xi,\psi=\text{const}) \approx \frac{1}{n_1}\sum_{i=1}^{n_1}\left\{\Phi_{n_1,i}(\xi)I(\xi_i,\psi)\right\},$$

$$\Phi_{n,i}(\xi) = 1+2\sum_{m=1}^{n-1}T_m(\xi_i)T_m(\xi) = \frac{T_{n-1}(\xi_i)T_n(\xi)}{\xi-\xi_i},$$

$$\xi_{\sigma i} = \cos\left[\frac{2i-1}{2n_1}\pi\right].$$

Now if we put $I_i(\psi) = I(\xi_i,\psi)$ and build a polynomial for $I_i(\psi)$ we derive that

$$I(\xi,\psi) \approx \frac{1}{n_1 n_2}\sum_{i=1}^{n_1}\left\{\Phi_{n_1,i}(\xi)\sum_{j=1}^{n_2}I(\xi_i,\psi_j)\Phi_{n_2,j}(\psi)\right\}.$$

Thus, if we have the integrals calculated at nodes ξ_i,ψ_j it is easy to obtain them at arbitrary points from $-1\le\xi,\psi\le 1$. There is a simple way to increase effectiveness of the integral's calculation. The other possibility to improve the quality of numerical algorithm is extracting the weight function in the Sommerfeld type integrals. If we know that

$I(\xi,\psi)=I^*(\xi,\psi)\omega(\xi,\psi)$, where $\omega(\xi,\psi)$ is known and well-calculated function (for example, $\omega(\xi,\psi)=\exp\left[i\chi\sqrt{\xi^2+\psi^2}\right]$) then the following formulae are useful:

$$I(\xi,\psi)\approx\omega(\xi,\psi)\frac{T_{n_1}(\xi)T_{n_2}(\psi)}{n_1 n_2}\sum_{i=1}^{n_1}\left\{\frac{1}{\xi-\xi_i}\times\right.$$

$$\left.\times\sum_{j=1}^{n_2}\frac{\tilde{I}(\xi_i,\psi_j)}{\psi-\psi_j}\right\},$$

$$\tilde{I}(\xi_i,\psi_j)=T_{n_1-1}(\xi_i)T_{n_2-1}(\psi_j)I^*(\xi_i,\psi_j).$$

As a test in Table 1 we would like to demonstrate some results of the free space Green function $H_0^{(1)}(x)$ interpolation by one-dimensional polynomial. We used 15 nodes on the interval x=[1;41].

Table 1.

x	$H_0^{(1)}(x)$	Absolute error for $\omega(\xi)=1$	Absolute error for $\omega(\xi)=\exp[ix]$
5	(–0.177597, -0.308518)	0.199068	0.001137
9	(–0.090334, 0.249937)	0.092254	0.000203
13	(0.206926, -0.078208)	0.015398	0.000018
17	(–0.169854, -0.092637)	0.041813	0.000033
21	(0.036579, 0.170202)	0.122417	0.000081
25	(0.096267, -0.127249)	0.170105	0.000115
29	(–0.147849, 0.009481)	0.143034	0.000116
33	(0.097271, 0.099135)	0.062674	0.000071
37	(0.010862, -0.130715)	0.038804	0.000069

Thus the simple weight function extracting before interpolation leads to essential decrease of calculation error.

Integral equations of the problem

In the case of homogeneous slab ($\varepsilon_2=\varepsilon_0$, $\mu_2=\mu_0$) we present the total diffracting field as a single layer potential

$$E(z)=E^*(z)+2\pi\sum_{k=1}^{N}\int_{L_k}j_k(t_k)G^E(t_k,z)ds_k \qquad (6)$$

for E-polarization or as a double layer potential

$$H(z)=H^*(z)+2\pi\sum_{k=1}^{N}\int_{L_k}m_k(t_k)\frac{\partial}{\partial n_k}G^H(t_k,z)ds_k \qquad (7)$$

in the case of H-polarization. Here the variable $z=x+iy$ denotes complex coordinate of observation point, $j_k(t_k)$ and $m_k(t_k)$ are unknown functions proportional to the surface current densities induced on screens by excitation wave, n_k is a normal to the contour L_k, $\partial/\partial n_k$ marks a partial derivative by normal at the internal point $t_k=x_k+iy_k$ with arc abscissa s_k of contour L_k.

When $\varepsilon_2\neq\varepsilon_0$ and $\mu_2\neq\mu_0$ we can present the total diffracting field as

$$E(z)=E^*(z)+2\pi\sum_{k=1}^{N}\int_{L_k}j_k(t_k)G^E(t_k,z)ds_k+$$

$$+2\pi\int_{L_0}j_0(t_0)G^E(t_0,z)ds_0, \qquad (8)$$

in the case of E-polarization or like

$$H(z)=H^*(z)+2\pi\sum_{k=1}^{N}\int_{L_k}m_k(t_k)\frac{\partial}{\partial n_k}G^H(t_k,z)ds_k+$$

$$+2\pi\int_{L_0}j_0(t_0)G^H(t_0,z)ds_0 \qquad (9)$$

for the H-polarized excitation.

Note, that in the case of periodic problem the presentations of a total diffracting field are similar to (6) and (7) with appropriate (according to polarization) Green functions.

Taking into account that the Green functions satisfy specific to the problem conditions all what we need it is to satisfy the boundary condition on the screens (contours L_k, $k=\overline{1,N}$). Doing it we obtain different (depending on polarization) system of integral equations. Their kernels consist logarithmic singularity, Cauchy type singularity or hyper-singularity [37,38,42]. The Meixner edge condition as a matter of fact defines the classes of such systems solution.

Let us consider some general forms of such integral equations. One of them is weak singular (logarithmic) integral equation of the first kind. It looks like

$$-\int_{-1}^{1} j(x)\ln|x-y|/\sqrt{1-x^2}\,dx +$$

$$+\int_{-1}^{1} j(x)K(x,y)/\sqrt{1-x^2}\,dx = -E(y).$$

If we apply a traditional regularization to the first term we obtain equation in the following form

$$\pi j(y)\ln 2 - \int_{-1}^{1}[j(x)-j(y)]\ln|x-y|/\sqrt{1-x^2}\,dx +$$

$$+\int_{-1}^{1} j(x)K(x,y)/\sqrt{1-x^2}\,dx = -E(y), \qquad (10)$$

$y\in[-1;1]$

Now, we assume that all regular functions (also unknown function) can be represented by interpolation polynomial as follows

$$f(x)\approx\frac{1}{n}\sum_{k=1}^{n} f(x_k)\Phi_{n,k}(x), \qquad (11)$$

$$x_k=\cos\varphi_k,\quad \varphi_k=\frac{2k-1}{2n}\pi,\quad n>1.$$

Now we apply the familiar Gaussian quadrature formula

$$\int_{-1}^{1} f(x)/\sqrt{1-x^2}\,dx=\frac{\pi}{n}\sum_{k=1}^{n} f(x_k), \qquad (12)$$

and obtain a numerical analog of integral equation (10):

$$\pi j(y)\ln 2-\frac{\pi}{n}\sum_{k=1}^{n}\left[j(x_k)-j(y)\right]\ln|x_k-y|+$$

$$+\frac{\pi}{n}\sum_{k=1}^{n} j(x_k)K(x_k,y)=-E(y),\ y\in[-1;1]. \qquad (13)$$

Now assume that derivative $j'(y)$ is finite on the interval [-1;1] (due to Meixner edge condition this assumption is obeyed always in the scalar diffraction theory). Let us put y equal to nulls of the Chebyshev polynomial of the first kind. We derive that

$$\frac{\pi}{n} j(y_l)\left[n\ln 2+\sum_{\substack{k=1\\k\neq l}}^{n}\ln|x_k-y_l|\right]-$$

$$-\frac{\pi}{n}\sum_{\substack{k=1\\k\neq l}}^{n} j(x_k)\ln|x_k-y_l|+\frac{\pi}{n}\sum_{k=1}^{n} j(x_k)K(x_k,y_l)=$$

$$=-E(y_l),\ y_l=\cos\left(\frac{2l-1}{2n}\pi\right),\ l=\overline{1,n}, \qquad (14)$$

or

$$\frac{\pi}{n}\sum_{k=1}^{n} j(x_k)\left[S(x_k,y_l)+K(x_k,y_l)\right]=-E(y_l),$$

$$S(x_k,y_l)=\begin{cases} n\ln 2+\sum\limits_{\substack{i=1\\i\neq l}}^{n}\ln|x_i-y_l|, & l=k;\\ -\ln|x_k-y_l|, & l\neq k.\end{cases} \qquad (15)$$

Now we have just to solve the system of linear algebraic equations (15). Scattering field we find via applying quadrature formula (12) to the presentations (6) or (8).

The second form of integral equation appears in the case of H-polarization. It looks like

$$\int_{-1}^{1} m(x)/(x-y)^2\,dx+\int_{-1}^{1} m(x)\ln|x-y|dx+$$

$$+\int_{-1}^{1} m(x)L(x,y)dx=F(y),\quad -1\le y\le 1. \qquad (16)$$

Here kernel $L(x,y)$, right-hand part $F(y)$ as well as unknown density $m(x)$ are regular functions which have continued first derivations.

Due to the Meixner edge condition we have $m(\pm1)=0$. Then (16) is equivalent [42] to

$$\int_{-1}^{1} m'(x)/(x-y)dx+\int_{-1}^{1} m(x)\ln|x-y|dx+$$

$$+\int_{-1}^{1} m(x)L(x,y)dx=F(y),\quad -1\le y\le 1. \qquad (17)$$

To solve this equation we present the unknown function as an interpolation polynomial with nodes as zeros of the second kind Chebyshev polynomials:

$$m(\xi)\approx\frac{2}{n+1}\sum_{i=1}^{n_1}\left\{P_{n_1,i}(\xi)m(\xi_i)\right\},$$

$$P_{n,i}(\xi)=\sum_{m=1}^{n}\sin(m\xi_i)\sin(m\arccos(\xi)),$$

$$\xi_i=\cos\theta_i,\quad \theta_i=\frac{i}{n+1}\pi.$$

Differentiating of the both sides of the last presentation yields

$$m'(x)\approx\frac{2}{n+1}\sum_{k=1}^{n} m(x_k)P'_{n,k}(x),$$

$$P'_{n_1 i}(\xi)=\sum_{m=1}^{n-1}\sin(m\xi_i)\frac{d\sin(m\arccos(\xi))}{d\xi}=$$

$$=-\sum_{m=1}^{n-1} m\sin(m\xi_i)\frac{\cos(m\arccos(\xi))}{\sqrt{1-\xi^2}}.$$

Taking into account the above formulae we can easy calculate the following singular integral

$$\int_{-1}^{1} m'(\xi)/(\xi-\xi_0)d\xi \approx -\frac{2}{n+1}\sum_{k=1}^{n} m(\xi_k)\times$$

$$\times\sum_{m=1}^{n-1} m\sin(m\xi_k)\int_{-1}^{1}\frac{\cos(m\arccos(\xi))}{\sqrt{1-\xi^2}}d\xi =$$

$$=\frac{\pi}{n+1}\sum_{k=1}^{n} m(\xi_k)\times\frac{S(\xi_k,\xi_0)}{\sqrt{1-\xi_0^2}};$$

$$S(\xi_k,\xi_0)=\sum_{m=1}^{n} m\cos\left(m(\theta_k-\theta)\right)-$$

$$-\sum_{m=1}^{n} m\cos\left(m(\theta_k+\theta)\right).$$

In particular case, when $\theta=\theta_l$, $l=\overline{1,n}$, we get the following relation

$$S(\xi_l,\xi_l)=(n+1)^2/2;$$

$$S(\xi_k,\xi_l)=\frac{1}{2}\left[\operatorname{ctg}^2\left(\frac{\theta_k+\theta_l}{2}\right)-\right.$$

$$\left.-\operatorname{ctg}^2\left(\frac{\theta_k+(-1)^{k-l}\theta_l}{2}\right)\right],\quad k\neq l.$$

As a result we obtain an interpolation type quadrature formula for calculation of the first term in equation (16).

To calculate the integral with logarithmic singularity in equation (16) we use the following transformation

$$\int_{-1}^{1} m(\xi)\ln|\xi-\xi_0|d\xi =$$

$$=\frac{2}{n+1}\sum_{i=1}^{n_1}\left\{m(\xi_i)\int_{-1}^{1}P_{n_1,i}(\xi)\ln|\xi-\xi_0|d\xi\right\}=$$

$$=\frac{2}{n+1}\sum_{i=1}^{n_1}\left\{m(\xi_i)\sin(m\xi_i)\times\right.$$

$$\left.\times\int_{-1}^{1}\sin(m\arccos(\xi))\ln|\xi-\xi_0|d\xi\right\}=$$

$$=\frac{-\pi}{n+1}\sum_{i=1}^{n} m(\xi_i)\left\{\sin\theta_i\left[\ln 2-\frac{T_2(\xi_0)}{2}\right]+\right.$$

$$\left.+\sum_{k=1}^{n}\sin(k\theta_i)\left[\frac{T_{k-1}(\xi_0)}{k-1}-\frac{T_{k+1}(\xi_0)}{k+1}\right]\right\}.$$

To calculate the regular integral we use well known Gaussian quadrature formula in the following form

$$\int_{-1}^{1}\sqrt{1-\xi^2}\,m(\xi)d\xi=\frac{\pi}{n+1}\sum_{i=1}^{n}\sin^2\theta_i m(\xi_i).$$

We reduce the integral-differential equation (16) to a system of linear algebraic equations using the method of mechanical quadratures. The essence of this approach consists in numerical treatment of the integral equation (16) by application of the above mentioned quadrature rules. Note, that a rigorous mathematical justification of this approach is performed (see for example [43]). After solving the linear algebraic system we evaluate the unknown density $m(\xi)$ using formula (17).

Results and simulations

a) Screens in open planar waveguide

Let's apply the numerical method of diffraction problem solution expounded in the previous sections to determine the field on the interface $y=0$ and at $x\to\pm\infty$ (wave zone or far-field pattern) [37]. We consider the particular case when the excitation is normal incident plane wave

$$W^*(z)=\exp[-i\chi_1\Im\{z\}] \qquad (18)$$

or own waveguide mode

$$W^*(z)=\left\{\begin{matrix}\cos\\ \sin\end{matrix}\right\}(p_k\chi_2(y-d/2))\exp[ih_k\chi_2 x], \qquad (19)$$

$-d\le y\le 0$, $\chi_1=\chi_3$.

Here $2\pi/(h_k\chi_2)$ is the k-th waveguide mode wavelength; $p_k=\sqrt{\varepsilon_2^2-\chi_2^2}$, symbol ε denotes dielectric constants of the media.

Let the relations $\varepsilon_1/\varepsilon_2=0.25$, $d=\lambda$, $a=\lambda/10$ occur. The single metallic strip $-a\le x\le a$ is situated horizontally in the slab at $y=-d/2$. It is interesting how the thickness and the slab material properties influence the scattered electromagnetic field. In Fig. 8 and Fig. 9 we present the magnitude and phase dependencies for scattered field in the case of E-polarized plane wave excitation.

The designations 1-3 in Fig. 8 correspond to $\varepsilon_3/\varepsilon_2=0.64$; 1; 1.44. From this figure we notice that the magnitude of the field electric component substantially decreases and its phase is practically unchanged with increasing ε_3. Observe that in $\varepsilon_3/\varepsilon_2=0.64$ case the non-attenuated waves arise in the slab. The designations 1-3 at Fig. 9 correspond to $d=0.7\lambda$; 1.1λ; 1.5λ and $\varepsilon_3/\varepsilon_2=0.64$. As indicated in the picture a slab thickness substantially (more than 50 %) changes the scattered

field magnitude. The corresponding phase of electric component changes on thickness by almost 5 % and less. Consequently, under slight variation both of the layer thickness and dielectric constant of underlying half-space the scattered wave amplitude undergoes substantial changes too. Its phase remains almost invariant in this case. Due to the phase curves we can detect a screen as well as determine the depth of its location.

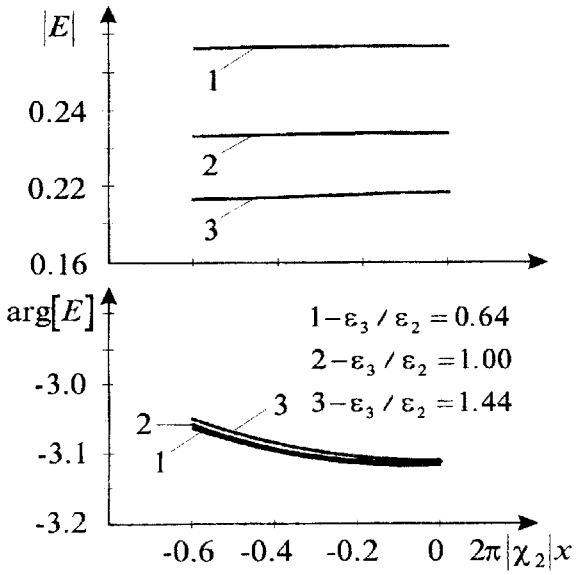

Fig. 8. *The magnitude and phase dependencies at different dielectric constants of the underlying half-space (the case of plane E-wave scattering)*

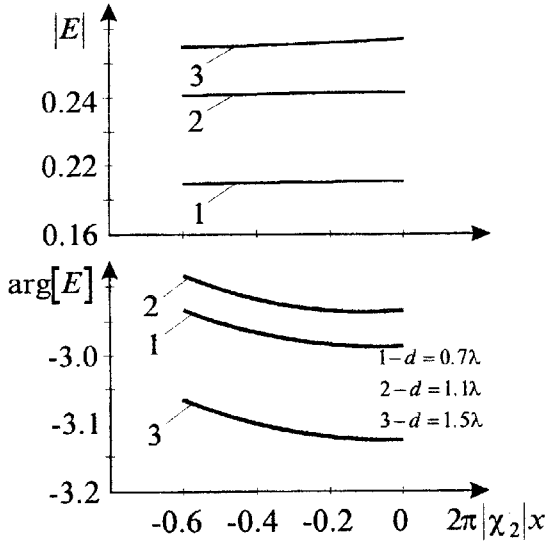

Fig. 9. *The magnitude and phase dependencies at different slab thickness (the case of plane E–wave scattering)*

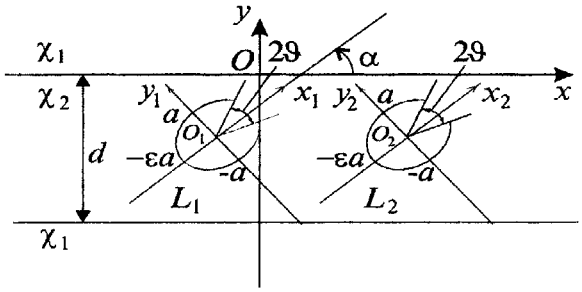

Fig. 10. *Cross-section of elliptical screens in the planar waveguide*

The numerical results given in the Fig. 11-Fig. 19 correspond to the configuration shown in Fig. 10 at $\chi_2/\chi_1=1.5$; $\chi_2 d=3$.

Calculations were carried out during slab illumination both by E- and H-polarized non-attenuated planar waveguide mode. We consider the transmission T_{jk} $(x\to+\infty)$ and reflection R_{jk} $(x\to-\infty)$ coefficients of such waveguide modes which are specified by formula

$$W(z)-W^*(z)=\Psi_j(\varphi)\left(\frac{2}{i\pi\chi_2 r}\right)^{1/2}\exp(i\chi_2 r)+$$

$$+\sum_{k=1}^{n_p}\begin{Bmatrix}T_{jk}-\delta_{jk}, x>0\\ R_{jk}, \quad x<0\end{Bmatrix}\begin{Bmatrix}\cos\\ \sin\end{Bmatrix}p_k\chi_2 y e^{ih_k\chi_2|x|}, \quad (20)$$

where δ_{jk} is Kronecker delta symbol; Ψ_j is far-field pattern; $n_p\geq 1$ is number of non-attenuated waveguide modes; $1\leq j\leq n_p$ is an index of the exciting waveguide mode. In the simplest case (see formula (20)) we have $j=n_p=1$, $T_{11}\equiv T$, $R_{11}\equiv R$. In the slab (region S_2) and at the single-mode excitation the squares of these coefficients define respectively the transmitted $(P^t=|T|^2P^{inc})$, reflected $(P^r=|R|^2P^{inc})$ as well as dissipated $(E/P^{inc}=1-|T|^2-|R|^2)$ field energy normalized by the incident mode power P^{inc}.

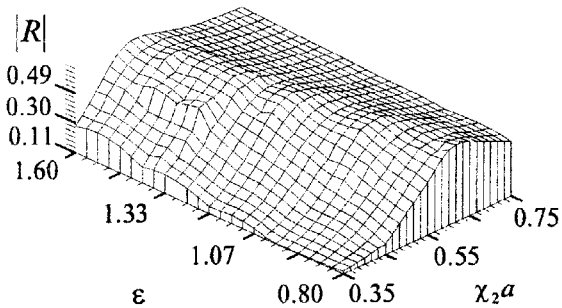

Fig. 11. *The H-polarized waveguide mode reflection as screen curvature ε and size $\chi_2 a$ function*

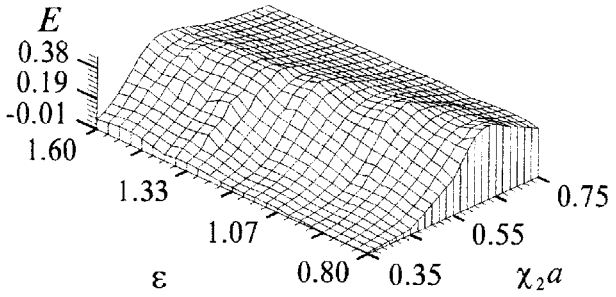

Fig. 12. *The H-polarized wave energy dissipation as screen curvature ε and size $\chi_2 a$ function*

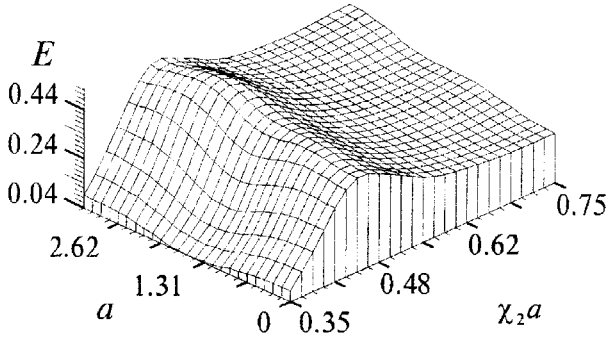

Fig. 13. *The H-polarized wave energy dissipation as function of screen orientation and size*

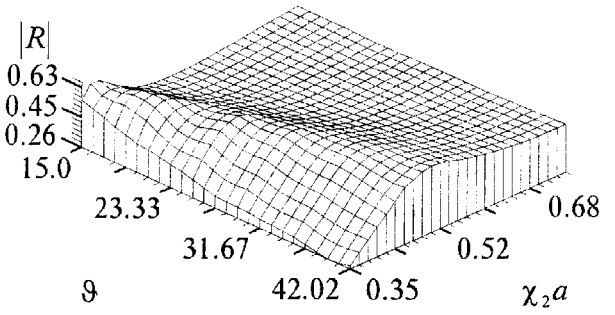

Fig. 14. *The H-polarized waveguide mode reflection as function of screen slot' width and size*

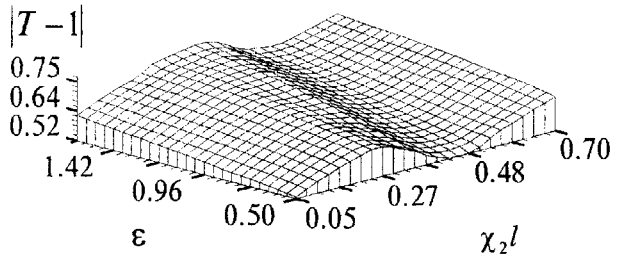

Fig. 15. *The E-polarized waveguide mode transmission as screen curvature ε and distance $\chi_2 l$ function*

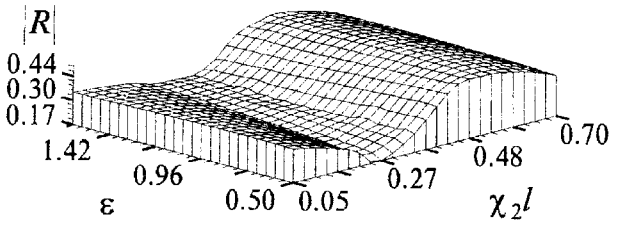

Fig. 16. *The E-polarized waveguide mode reflection as screen curvature ε and distance $\chi_2 l$ function*

Let the equations of contours L_k, k=1,2 are represented parametrically by formula

$$t_k(\tau) = a\cos([\pi - \vartheta]\tau) + i\varepsilon\cos([\pi - \vartheta]\tau)e^{i\alpha} - -id/2 + (2a + l)(k-1), \quad -1 \le \tau \le 1. \qquad (21)$$

Here a and εa are the ellipses half-axis; l is a distance between screens; 2ϑ is an angular size of the screen slot; α is an angle of screen orientation relative to the y=0 plane. Calculations were performed bearing in mind that $\chi_2 a$=0.35, $\alpha=\pi/2$, $\vartheta=\pi$ in the case of E-polarization and $\alpha=\pi/6$, $\vartheta=\pi/6$, ε=0.6 at H-polarized excitation.

Referring to Fig. 11 and Fig. 12 we can see the function's resonant behavior in the domain $0.35 \le \chi_2 a \le 0.7$. The resonance frequency and resonance merit factor increase when ε reduces. In Fig. 13 the dependence of dissipation energy is shown graphically as the function of orientation angle and screen size $\chi_2 a$. Here ε=1.6; $\vartheta=\pi/6$. From this figure we notice that the resonance appears at different wave size of the screen depending on its orientation in the slab. Consequently, the screen orientation in the case of its H-polarized excitation produces a significant change in the scattered field. As is shown in Fig. 14 (here we put ε=1.6; $\alpha=\pi$) the resonance frequency increases when the slot aperture extends. Note, that the corresponding merit factor decreases in this case.

The E-polarized wave transmission and reflection coefficients as functions of distance between screens $\chi_2 l$ and their curvature ε are shown in Fig. 15 and Fig. 16. The functions maxima depend on distance between screens as well as on parameter ε (according to (21) the change of curvature ε is equivalent to the change of screens size). Note that location of the functions' maxima slightly depends on ε. For small curvature ε we observe the transmission maximum at $l \approx 0.4\lambda$ and minimum at

$l \approx 0.27\lambda$ (λ - is a wavelength). The growth of screen's size causes shift of the functions $|T\text{-}1|$ and $|R|$ extremes to the high frequency range. The results of the *H*-polarized scattered field calculations as function of distance $\chi_2 l$ and screen's size $\chi_2 a$ are illustrated in Fig. 17 - Fig. 19.

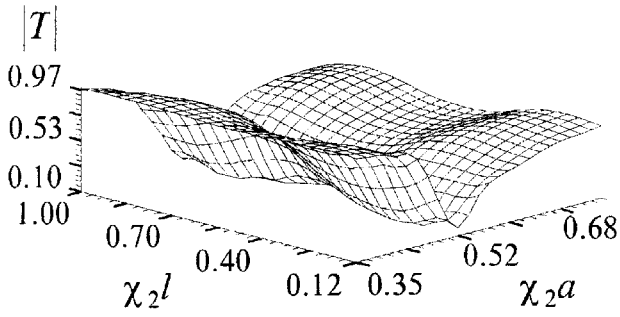

Fig. 17. *The H-polarized waveguide mode transmission as screen size $\chi_2 a$ and distance $\chi_2 l$ function*

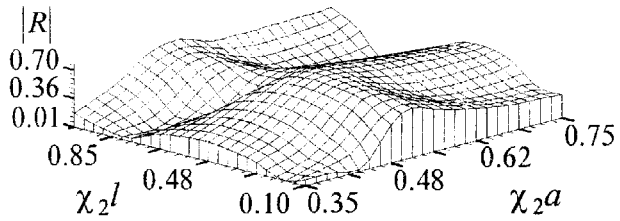

Fig. 18. *The H-polarized waveguide mode reflection as screen size $\chi_2 a$ and distance $\chi_2 l$ function*

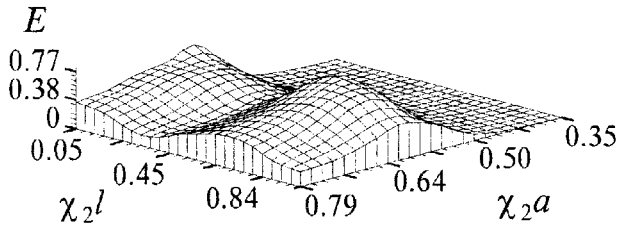

Fig. 19. *The H-polarized wave energy dissipation as the function of distance $\chi_2 l$ and size $\chi_2 a$*

We see that value $\chi_2 a=0.52$ which corresponds to the resonant size of each screen remains extreme in the case of their system. The resonance amplitude depends on the distance between screens slightly. The largest and the smallest transmission coefficient values are achieved at $\chi_2 a=0.48$ and $\chi_2 a=0.21$. The transmission resonance at $l \approx 0.48\lambda$ corresponds to waves multiply reflected by screens system. The resonance amplitude depends on the screens size only if $\chi_2 a \le 0.55$. The corresponding analysis of energy dissipation (Fig. 19) shows that the single slotted screen resonance is the reason of powerful energy dissipation and the screens system decreases this losses.

The above calculations demonstrate the possibility of suggested approach to the accurate determination of electromagnetic field scattered by system of cylindrical screens in slab. The geometrical and physical parameters in the problem are supposed to be arbitrary. The developed numerical schemes in fast acting and on-line request memory can analyze the scattering on screens up to few tens of λ by the modern personal computers. Coupled with accuracy of obtained results the above confirms the high effectiveness of the approach and wide areas of its application.

b) Gratings

For testing of the obtained results let us solve a simplest problem of plane wave reflection by infinite plane screen in the case of normal illumination. It is obvious that this problem can be reduced to the following integral equation

$$\frac{\pi i}{2} j \int_{-\infty}^{+\infty} H_0^{(1)}(\chi r)dx = -E^*(x_0). \qquad (22)$$

Taking into account the value of the following integral [44]

$$\int_{-\infty}^{+\infty} H_0^{(1)}(\chi r)dx = 2\int_0^{+\infty} H_0^{(1)}(\chi r)dx = \frac{2}{\chi}, \qquad (23)$$

from equation (22) we easily obtain next relation for current density:

$$\frac{\pi i}{2} j \frac{2}{\chi} = -E^*(x_0). \qquad (24)$$

If we assume here $\chi=1$, $E^*(x_0)\equiv 1$, then we obtain that

$$j = i/\pi. \qquad (25)$$

Now divide our plane screen on infinite periodic system of strips. Each strip has width $2a$ (see Fig. 20). Let us consider this system as a grating. Assume $\chi d=\pi$, $2\chi a=\pi$ and solve this problem numerically. Also, an infinite screen was considered as a grating with two the same strips within period. In this case the strip's width was $2\chi a=\pi/2$. The accuracy of solution within 0.01 % we achieve with 15 collocation nodes per wavelength. The check was carried out also with some numerical

results in partial case of single element diffraction grating with screens of constant [28,30] or of variable [29] curvature.

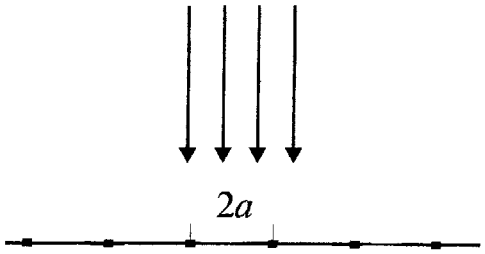

Fig. 20. *Infinite screen as a periodic system of strips*

As an example let us consider the case when two screens are situated on the gratings' period [45]. Suppose, that contours L_k are parabolic arcs with their endpoints $\pm a+il(k\text{-}1)$ and tops at the points $ib+il(k\text{-}1)$ (Fig. 21).

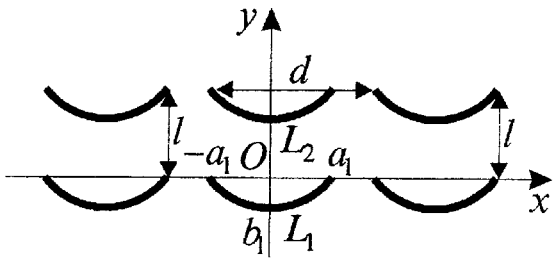

Fig. 21. *Infinite two-element grating*

Let us introduce complex value equations of arcs L_k in the following form

$$t_k(\tau) = a\left(\tau + i\varepsilon_k\left(1-\tau^2\right)\right) + il(k-1), \qquad (26)$$

$$\varepsilon_k = \varepsilon = b/a,\ \tau = [-1;1],\quad k = 1,2.$$

Here l is a distance between screens in cascade. Grating is illuminated by E-polarized plane wave with incidence angle β=0. The wave number χ is assumed to be real.

An influence of geometric parameters of the cascade screens system on the induced currents has been investigated for the cases $\chi d=\pi$, $\chi a=\pi/4$ (Fig. 22).

We see that distance between screens makes an essential influence on the current's magnitude. For value l that is divisible by half length of excitation wave, we find resonance (here ε=0.5). An influence of curvature of screens was established on magnitude of currents that are induced on the illuminated screen (contour L_2) for resonance distance l=0.5λ, $\lambda=2\pi/\chi$ (Fig. 23).

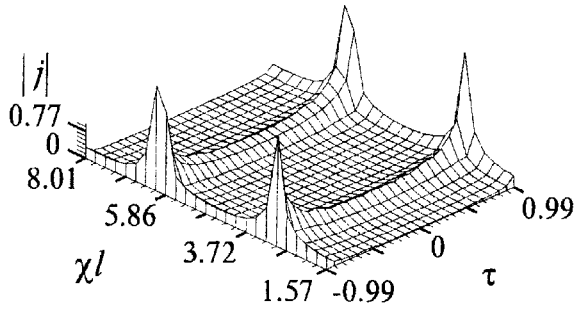

Fig. 22. *An influence of distance l on shadow screen's current*

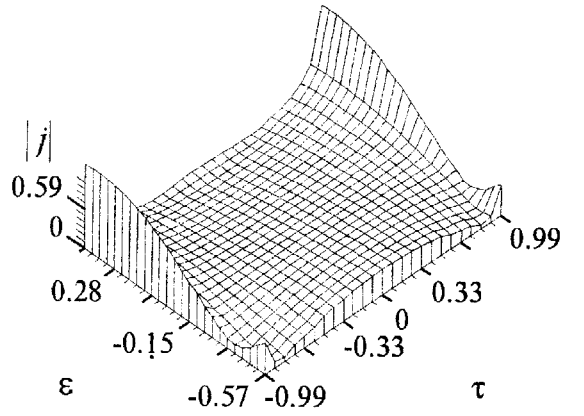

Fig. 23. *An influence of curvature ε on illuminated screen's current*

Currents depend also on profile of the screens. In particular at $\varepsilon = 0.4$, the magnitude of current at screen's ribs tends to zero.

Note, that infinite two element gratings (see Fig. 21) can be considered as an open planar waveguide. It is found that at certain distances l this structure may be transparent for electromagnetic waves with wavelength almost equal to period of the gratings.

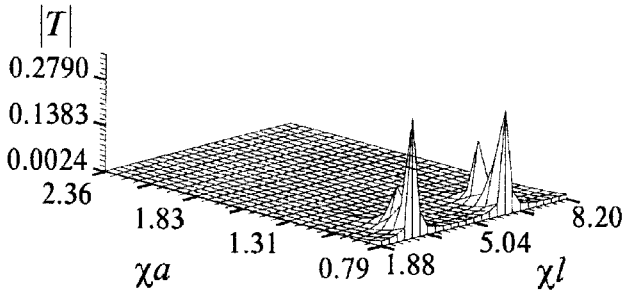

Fig. 24. *Transmission coefficient for two element plane grating (ε=0)*

Let us consider the transmission coefficient of electromagnetic wave for two-elements cascade gratings with strip as an element (Fig. 24). At distances l, which

corresponds to appearance of additional modes of planar waveguide the transmission coefficient is maximal. This resonance distance depends also on size of the screens. In other words, for low density of gratings filling the waveguide becomes wider. When increasing density of filling ($\chi a \to \pi/2$) we increase reflection properties of upper layer of screens so we decrease transmission of waves.

On the Fig. 25 and Fig. 26 the transmission coefficients for concave-out ($\varepsilon_1=\varepsilon>0$, $\varepsilon_2=-\varepsilon<0$) and concave-in ($\varepsilon_1=-\varepsilon<0$, $\varepsilon_2=\varepsilon>0$) screens are presented.

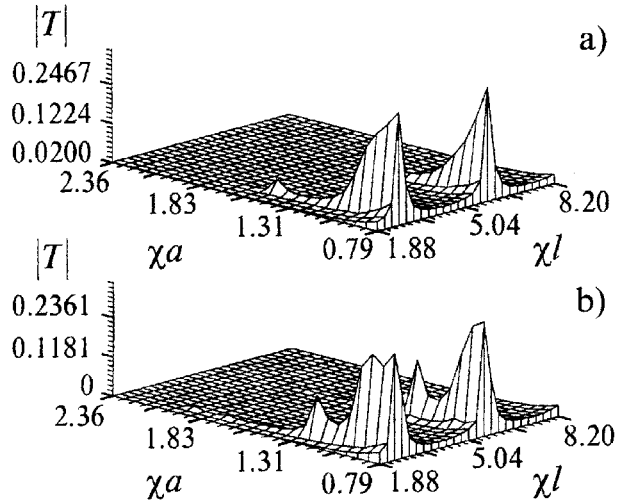

Fig. 25. *Transmission coefficient for different screen's curvature: a*)ε=0.25; *б*)ε=0.5

We see that the curvature of screens influences the physical properties of cascade grating. The screen's curvature changes an influence of density filling of multilayer grating on the wave transmission. For slightly curved screens the transmission is possible only for small filling of array. For essentially curvilinear grating's elements the effect of transparency appears for higher density of gratings filling (Fig. 25b, Fig. 26b, $\chi a \approx 1.83$). The higher curvature causes increase of transparency (the magnitude of waves which transmit through structure is significant). (Fig. 25b, Fig. 26b).

For testing obtained numerical results, we specially investigated their stability and convergence at resonance frequencies. Taking into account of high merit factor of the effects that we considered such investigation to our opinion is obligatory. Note, that the determinant of algebraic system (that is obtained by mechanical quadratures method) dramatically decreases at resonance frequencies. Nevertheless, calculation of Green function with relative error $\delta=10^{-5}$ for gratings with parameters $\chi\lambda \approx 2\pi$; $\chi a \approx 1.47$; $\varepsilon=0.25$; $N=2$ ensures an error no more than 0.1 % in the resonance transmission coefficients. Such accuracy was established at number of quadratures formula nodes equal to 35. The same investigations were performed for all resonance cases presented in this work. It allows us to affirm reliability of effects described above.

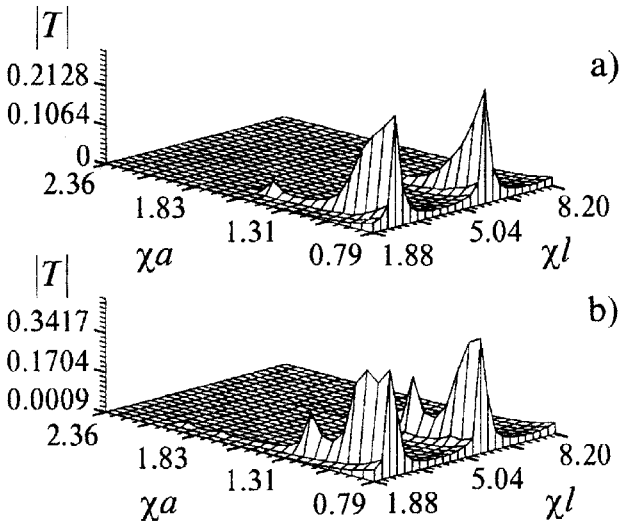

Fig. 26. *Transmission coefficient for different screen's curvature: a*)ε=–0.25; *b*)ε=–0.5

Conclusion

The integral presentation of periodic Green function supposed here allows to increase an accuracy of calculation essentially. Applying of interpolation polynomial for its approximation substantially decrease the time of calculation. It allowed us to construct an effective numerical algorithm for solution of wide class of scalar scattering problems. The accuracy of this approach in the resonance frequency range is close to the accuracy of rigorous numerical-analytical technique [28,30,31,34]. At the same time the numerical treatment of the singular integral equations allows to study the electromagnetic field properties without any restrictions on shape of the screens and their location.

References

1. Ch. Butler. Radio Sci. 1987, **22**, No. 7, pp. 1149-1154.
2. L. Chammeloux, Ch. Pichot and J.-Ch. Bolomey. IEEE Trans. on Microwave Theory and Techniques. 1986, **MTT-34**, No. 10, pp. 1064-1076.

3. Hongo Kohei and Hamamura Akihiko.IEEE Trans. on Antennas and Propagation. 1986, **AP-34**, No 1, pp. 1306-1312.
4. E. I. Nefedov and A. T. Fialkovskii. Strip-line transmission: electrodynamic foundation of SHF integrated circuits automatic designing. Moscow, Nauka, 1980 (in Russian).
5. V. I. Dmitriev.Vychisl. met. program. 1965, **3**, pp. 207-316 (in Russian).
6. L. A. Tabarovsky. Application of the integral equations method in geoelectrical problems. Novosibirsk, Nauka, 1975 (in Russian).
7. N. K. Uzunoglu and J. D. Kannelopoulos. J. Phys. A: Math. and Gen. 1982, **15**, No. 2, pp. 459-471.
8. V. V. Sukhorukov. Mathematical modeling of electromagnetic fields in conducting bodies. Moscow, Energia, 1976 (in Russian).
9. A. L. Dorofeev and Yu. G. Kazamanov. Electromagnetic non-destructive testing. Moscow, Mashinostroienie. (in Russian).
10. X. B. Xu and Ch. Butler. IEEE Transaction on Antennas and Propagation. 1986, **AP-34**, No. 7, pp. 880-890.
11. X. B. Xu and Ch. Butler. Ibid. 1987, **AP-35**, No. 5, pp. 529-539.
12. N. Morita. IEEE Proc. 1980, **H127**, No. 5, pp. 263-269.
13. N. K. Uzunoglu and J. G. Fikioris. J. Opt. Soc. of America. 1992, **72**, No. 5, pp. 628-637.
14. A. G. Yarovoy. Akustichesky Zhurnal. 1992, **38**, No. 4, pp. 756-763 (in Russian).
15. N.P. Zhuk and S.B. Shulga. Radiotekhnika (Kharkiv). 1989, **90**, pp. 93-101 (in Russian).
16. K. A. Michalski and Ch. Butler. Radio Sci. 1988, **18**, No. 6, pp. 1195-1206.
17. Yu. V. Shestopalov. Reports of International Conference on Millimeter and Sub-millimeter Waves and Applications. San Diego, USA, January 10-14, 1994.
18. A. I. Nosich and V. P. Shestopalov. Dokl. Akad. Nauk SSSR. 1990, **311**, No. 5, pp. 1110-1115 (in Russian).
19. A. S. Andrenko and A. I. Nosich. Dokl. Akad. Nauk Ukr. SSR. 1989, **Ser. A**, No. 4, pp. 61-66 (in Russian).
20. A. I. Nosich. Analytical and Numerical Methods in Electromagnetic Wave Theory. Ed. M. Hashimoto, M. Idemen and O. Tretyakov. Tokyo, Science House Co., 1993, pp. 419-471.
21. J.-F. Zurcher and F. E. Gardiol. Broadband Patch Antennas. Norwood, MA, USA, Artech, 1995.
22. F. E. Gardiol. Microstrip Circuits. New York, John Wiley, 1994.
23. J. R. Mosig. IEEE Trans. on Microwave Theory and Techniques. 1988, **MTT-36**, pp. 314-323.
24. T. K. Sarkar and E. Arvas. IEEE Trans. on Antennas and Propagation. 1990, **AP-38**, pp. 305-312.
25. K. A. Michalski and J. R. Mosig. Electromagnetics. 1995, **15**, pp. 377-392.
26. F. E. Gardiol. Reports of 6th International Conference on Mathematical Methods in Electromagnetic Theory. Lviv, Ukraine, September 10-13, 1996.
27. R. F. Harrington. Field Computation by a Moment Method. New York, Macmillan, 1968.
28. V. P. Shestopalov, L. N. Litvinenko, S. A. Masalov and V. G. Sologub. Diffraction of waves on gratings. Kharkiv, Kharkiv University Publ., 1973 (in Russian).
29. V. V. Panasyuk, M. P. Savruk and Z. T. Nazarchuk. Method of singular integral equations in two-dimensional diffraction problems. Kyiv, Naukova Dumka, 1984 (in Russian).
30. V. P. Shestopalov. Method of Riemann-Hilbert problem in the theory of diffraction and propagation of electromagnetic waves. Kharkiv, Kharkiv University Publ., 1971 (in Russian).
31. V. P. Shestopalov and Yu. K Sirenko. Dynamic theory of gratings. Kyiv, Naukova Dumka, 1991 (in Russian).
32. R. Petit. Electromagnetic theory of gratings. Berlin, Springer, 1980.
33. E. Lüneberg. In: Analytical and Numerical Methods in Electromagnetic Wave Theory. Ed. M. Hashimoto, M. Idemen and O. Tretyakov. Tokyo, Science House Co., 1993, pp. 317-372.
34. L. N. Litvinenko and S. L. Prosvirnin. Spectral operator of scattering in problems of diffraction on plane screens. Kyiv, Naukova Dumka, 1984 (in Russian).
35. Z. T. Nazarchuk. Numerical investigation of waves diffraction by cylindrical structures. Kyiv, Naukova Dumka, 1989 (in Russian).
36. O. I. Ovsyannikov. Reports of 1st International Conference on Information Technologies for Image Analysis and Pattern Recognition. Lviv, Ukraine, 1990, **2**, pp. 336-340.
37. Z. T. Nazarchuk and O. I. Ovsyannikov. Journal of Electromagnetic Waves and Application. 1994, **8**, No. 11, pp. 1481-1498.
38. Z. T. Nazarchuk and O. I. Ovsyannikov. Dop. of Ukrainian *NAS*. 1994, **Ser. A**, No. 7, pp. 79-84 (in Ukrainian).
39. Z. T. Nazarchuk and O. I. Ovsyannikov. Turkish Journal of Physics. 1996, **20**, No. 4, pp. 371-375.
40. T. J. Rivlin. Chebyshev polynomials. New York, John Wiley, 1990.
41. I. P. Natanson. The constructive theory of functions. Moscow-Leningrad, State Technical Publishing, 1949.
42. Z. Nazarchuk. Singular integral equations in diffraction theory. Lviv, Karpenko Physico-Mechanical Institute, 1994.

43. M. G. Akhmadiev and B. G. Gabdulkhaev. Moscow, VINITI, 1988, No. 1167-B88 (in Russian).
44. M. Abramovitz and I. A. Stegun (Editors). Handbook on special functions. Moscow, Nauka, 1979 (in Russian).
45. Z. T. Nazarchuk and O. I. Ovsyannikov. IEEE Transactions on Antennas and Propagation. 1997, **AP-45**, No. 1, pp. 15-19.

Об одном численном подходе к решению СИУ в теории дифракции

З. Назарчук, О. Овсянников

Рассмотрен эффективный численный подход к решению скалярных дифракционных задач для системы произвольных цилиндрических экранов. Предложенный метод решения задачи основан на прямом численном решении соответствующих сингулярных интегральных уравнений.

Про один числовий підхід до розв'язання СІУ в теорії дифракції

З. Назарчук, О. Овсянніков

Розглянуто ефективний числовий підхід до розв'язання скалярних дифракційних задач для системи довільних циліндричних екранів. Запропонований метод розв'язання задачі базується на прямому числовому розв'язку відповідних сингулярних інтегральних рівнянь.